Journal of Natural Sciences and Mathematics Research
J. Nat. Scien. & Math. Res. Vol. 11 No.1 (2025) 29-46
ISSN: 2460-4453 (Online); 2614-6487 (Printed)
Available online at http://journal.walisongo.ac.id/index.php/jnsmr

Risk analysis of air quality for parameters NO_2, SO_2, NH_3, and O_x from the area around fertilizer industries in Indonesia

Dante Alighiri[1,*], Naufaldi Bani Widodo[1], Ravely Adhitya Abdullah[1], Indah Putri Firnanda[1], and Apriliana Drastisianti[2]

[1]Chemistry Department, Faculty of Mathematics and Natural Sciences, Universitas Negeri Semarang, 50229 Central Java, Indonesia

[2]Department of Chemistry Education, Faculty of Sciences and Technology, Universitas Islam Negeri Walisongo Semarang, 50185 Central Java, Indonesia

[*]Corresponding author: dante_alighiri@mail.unnes.ac.id

ABSTRACT

Industrial zones with intensive human activities often experience air-quality degradation, particularly in areas surrounding fertilizer production facilities. This study analyzes the concentrations of nitrogen dioxide (NO_2), sulfur dioxide (SO_2), ammonia (NH_3), and oxidants (O_x) in the ambient air around fertilizer industries in Indonesia and evaluates their potential non-carcinogenic health risks. Air sampling was conducted using an InScienPro US-1012 impinger equipped with selective absorbent solutions. Pollutant concentrations were quantified using UV-Vis spectrophotometry based on the Griess–Saltzman method for NO_2, the pararosaniline method for SO_2, the indophenol method for NH_3, and the neutral buffer potassium iodide method for O_x. Concentrations were compared with national ambient air-quality standards. To strengthen the assessment, a quantitative health-risk evaluation was incorporated using the Hazard Quotient (HQ) and Hazard Index (HI), allowing for the interpretation of long-term exposure impacts. Results show that most pollutant concentrations were below regulatory limits; however, SO_2 levels at one sampling point and NH_3 levels near the production zone were elevated. The HQ–HI analysis revealed that SO_2 at the office-area sampling point (HQ = 0.794) and NH_3 inside the processing plant (HQ = 2.238) were the dominant contributors to cumulative exposure, with HI values exceeding 1 at both locations. These findings indicate potential non-carcinogenic risks for individuals chronically exposed in areas closest to emission sources. Overall, this study highlights the importance of continuous monitoring and risk-based evaluation to identify localised hotspots, inform mitigation strategies, and enhance emission control practices in fertiliser-industrial environments.

Keywords:
Air pollution; fertilizer industry; gaseous pollutants; health risk assessment; Hazard Index.

Introduction

Areas with high human activity intensity often suffer from poor air quality due to numerous sources of air pollutants. Globally, air pollution negatively impacts air quality and poses a substantial threat to public health. Approximately 4.2 million deaths annually are due to ambient air pollution (WHO, 2020). Morbidity and mortality from cardiovascular and respiratory causes, in particular, have been linked to particulate air pollution (Kelly & Fussell, 2015; Shah et al., 2015). For instance, regions near fertilizer factories are prone to significant air pollution because fertilizer processing releases numerous air pollutants throughout production, from manufacturing to decomposition and waste incineration (Alighiri et al., 2015; Priatmoko et al., 2024).

Workers from these industries who handle materials are aware of the risks associated with exposure to harmful elements. Exposure to these components can have short- and long-term effects on employees, including changes to the metabolism of several biological processes in the human body (Fowler et al., 1993; Bocato et al., 2019). People living near these fertiliser industries or working in such areas have a high risk of undetected exposure to fertiliser toxicity (Chheang et al., 2021; Arshad and Shanavas, 2013; Kuzmanovic et al., 2022). Several harmful chemicals are released into the air, water, and land due to manufacturing fertilizer in industries that cause health effects by the lethal and carcinogenic elements found in fertilizer (Secretariat and United Nations Environment Programme, 2000; Yousef et al., 2017; Lenart- Boroń and Boroń, 2014).

The production activities within fertilizer processing plants generate solid, liquid, and gaseous waste. Fertilizer plants contaminate water and air, emitting CO, NH_3, NO_x, and SO (Ghavam et al., 2021; Kalbarczyk et al., 2018). One such activity that produces air pollutants is using boilers to generate steam, where the combustion process releases pollutants like nitrogen dioxide (NO_2), sulfur dioxide (SO_2), and Ox. With humidity, NO can be converted into nitric acid (HNO_3) and SO_2, and if oxidants are available, into sulphuric acid (H_2SO_4). Acidic air pollution leads to the hydrolytic degradation of materials, causing significant damage (Larsen, 2000; Bowden & Brimblecombe, 2003; Vallero, 2008). Ox, as a strong oxidant, causes fading of dyes and pigments and induces an attack on organic materials (Salmon et al., 2000). Furthermore, stack emissions can increase local air pollution exposure and contribute to adverse health effects for nearby residents (Lee et al., 2021).

For example, urea production generates air pollutants such as ammonia (NH_3). Fertilizer production has many consequences as well. Ninety per cent of globally produced N fertilizers are ammonia (Theregowda et al., 2019). Besides that, the initial form is nitric oxide (NO), which is subsequently oxidized by oxygen (O_2) to NO_2 through high-temperature combustion in the atmosphere. NO_2 is one of the most widespread air pollutants today, playing a significant role in the formation of smog and acid precipitation (Hong et al., 2017).

Air pollutants like nitrogen dioxide (NO_2), sulfur dioxide (SO_2), ozone (O_3), and ammonia (NH_3) have detrimental effects on human health. The primary health issue they cause is respiratory system diseases, which can affect both workers and residents living near fertilizer plants. Potential health effects include irritation that leads to eye damage, lung epithelial cell damage, pneumonia (Sarudji, 2010; Zakaria and Azizah, 2013; Ji et al., 2015), tissue damage causing oxidative stress, and bronchoconstriction (Walford, 2013). NO_2 pollution results in pulmonary edema due to severe pneumonia, and upper airway obstruction can occur due to gradual bronchiolar damage (Sarudji, 2010). Exposure to SO_2 gas negatively impacts the respiratory system and lung function, leading to cough, chronic bronchitis, increased asthma symptoms, and excessive mucus production (Zakaria and Azizah, 2013). NH_3 gas irritates the skin, eyes, and respiratory system and disrupts environmental sustainability due to its pungent odour (Kastiyowati, 2001). Meanwhile, O_3 pollution causes asthma, eye, nose, and throat irritation and contributes to global warming by reacting with substances like chlorofluorocarbons (CFCs), leading to ozone depletion. Long-term observations of the atmosphere are keys to understanding the processes that affect atmospheric composition (Gong et al., 2017; Liang et al., 2018; Bellouin et al., 2020; Kumar et al., 2022), weather and climate (Liu et al., 2019). Air pollution contributes to climate change and harms various aspects of human activity (Roy, 2021).

Therefore, testing the air quality near fertilizer plants is crucial to ensure that the surrounding environment remains safe for nearby communities. Continuous monitoring enables the detection of hazardous substances in the ambient air, allowing for timely mitigation measures. These efforts are essential to ensure compliance with the Threshold Limit Values (TLVs) established in Indonesian Government Regulation No. 22/2021 and the Decree of the Minister of Environment (1996). Recent international studies have also shown that concentration-based assessments alone are often insufficient for characterizing potential health risks in industrial regions. As a result, quantitative health-risk approaches, particularly the Hazard Quotient (HQ) and Hazard Index (HI), have become important tools for evaluating long-term inhalation exposure, especially in areas affected by fertilizer production, combustion processes, and ammonia-handling activities. Applications of HQ–HI in multi-pollutant assessments across industrial and urban settings demonstrate that adverse health effects may arise even when pollutant concentrations remain below regulatory thresholds (Ababio et al., 2025; Abidin et al., 2025; Cai et al., 2025). Integrating HQ–HI into the present study enhances the analytical depth by linking measured concentrations of NO_2, SO_2, NH_3, and oxidants (Ox) with their potential non-carcinogenic health implications.

This study aims to analyze and characterize the spatial distribution of gaseous pollutants emitted from fertilizer-industry operations in Indonesia and to evaluate their associated non-carcinogenic health risks using HQ–HI.

Material and Methods

Material

The materials used such as sulfamic acid (NH_2SO_3H), formaldehyde (HCHO), glacial acetic acid (CH_3COOH), sulfanilic acid monohydrate, sodium nitroprusside ($Na_2Fe(Cn)_5NO.H_2O$), sodium hypochlorite (NaOCl), phenol (C_6H_5OH), ammonium chloride (NH_4Cl) were purchased from Merck, Germany. *N*-(1-naphthyl) ethylenediamine (NEDA), pararosaniline hydrochloride ($C_{19}H_{17}N_3.HCl$), and anhydrous sulfanilic acid ($H_2NC_6H_4SO_3H$ were purchased from Sigma-Aldrich. Distilled water, filter paper (Whatman), and sulfuric acid (H_2SO_4) were purchased from Brataco, Indonesia. The tools used are glassware (Pyrex), Impinger InScienPro US-1012, impinger test tube, spectrophotometer UV-Vis Shimadzu type UV-2600 (double beam), flowmeter, pump, and tripod.

Absorbent preparation of ambient air

The absorbent preparation of ambient air used in this study involves using an impinger containing an absorbent solution. The absorbent solution used for each test parameter is different, and these solutions are prepared according to the standard methods outlined in the Indonesian National Standard (SNI). The preparation method for the NO_2 absorbent solution follows SNI 7119-2-2017, the SO_2 absorbent solution follows SNI 7119-7:2017, the NH_3 absorbent solution follows SNI 19-7119.1-2017, and the O_x absorbent solution follows SNI 19-7119.8-2017 (SNI, 2017).

Sampling of ambient air

Sampling was conducted using the InScienPro US-1012 impinger at five different locations:

1. Point A at the industrial fertilizer product storage warehouse
2. Point B at the office area of the fertilizer industry
3. Point C inside the fertilizer processing plant
4. Point D at the entrance gate of the industrial area
5. Point E in a village surrounding the industrial area

Sampling was carried out after 11:00 AM, during active working hours of the fertilizer plant, ensuring the samples accurately represent actual conditions. For each sampling point, three replicate air samples were collected, resulting in a total of 15 samples for NO_2, SO_2, NH_3, and O_x measurements. Each replicate sample was transferred into an individual labeled sample container to maintain traceability and allow statistical comparison across locations.

Prior to sampling, the US-1012 impinger was assembled at a height of 1.5 meters above ground level to mimic human breathing and minimize physical obstruction. The impinger tubes were filled sequentially with selective absorbent solutions for NO_2, SO_2, NH_3, and O_x. The flow rates were adjusted to 0.4, 0.5, 1.2, and 1.2 L/min, respectively. Sampling duration was set to 60 minutes for NO_2, SO_2, and NH_3. For O_x, the absorbent solution was collected after the first 30 minutes and transferred to a dedicated container. Afterwards, the impinger tube was refilled with a fresh absorbent solution and sampling continued for the remaining time. This procedure ensured that two O_x samples per point (early and late capture) were obtained, increasing the accuracy of oxidant measurements.

Preparation of standard curve for NO_2, SO_2, NH_3, and O_x

The spectrophotometer was optimized, and standard solutions were prepared according to the respective SNI methods for NO_2, SO_2, NH_3, and O_x. Measurements were carried out at the maximum wavelength for each parameter: 550 nm for NO_2, 540 nm for SO_2, 630 nm for NH_3, and 352 nm for O_x. A 25 mL volumetric flask was prepared with one blank solution and seven standard solutions with proportionally different concentrations within the measurement range for each parameter. The lowest working standard solution was prepared close to the limit of quantitation (LoQ). A standard curve was created by plotting the absorbance against the concentration of the standard solutions.

Assay parameter for NO_2 dan O_x

The concentration of NO_2 and O_x in the samples was tested using a UV-Vis spectrophotometer at the maximum wavelengths of 550 nm for NO_2 and 352 nm for O_x. The absorbance of each sample was measured and then extrapolated to the linear equation from the standard curve to determine the concentrations of NO_2 and O_x in the samples.

Assay parameter for SO_2

The test sample was placed into a 25 mL volumetric flask, and 1 mL of 0.6% sulfamic acid solution was added. After waiting 10 minutes, 2 mL of 0.2% formaldehyde solution and 5 mL of pararosaniline solution were added. The flask was then homogenized and filled to the calibration mark with distilled water. The mixture was left to stand for 30 minutes before being measured with a UV-Vis spectrophotometer at a maximum wavelength of 540 nm. The concentration was then determined by extrapolating the measured absorbance onto the linear regression equation from the standard curve.

Assay parameter for NH_3

The test sample was transferred into a 25 mL volumetric flask. Sequentially, 2 mL of ammonia buffer solution, 5 mL of phenol reagent solution, and 2.5 mL of sodium hypochlorite reagent solution were added to each flask. The flask was then homogenized and filled to the calibration mark with distilled water. The mixture was allowed to stand for 30 minutes. The absorbance was read using a UV-Vis spectrophotometer, and the concentration was determined using the linear regression equation derived from the calibration curve of the standard solutions based on Lambert Beer's law.

Calculation of the concentration of pollutants in the ambient air

The concentration of gaseous pollutants in ambient air can be determined through further calculations by comparing the concentration in the sample with the volume of air sampled during collection. The volume of the sampled air corrected standard conditions (25°C, 760 mmHg) can be calculated using the following formula:

$$V = \frac{\sum_{i=1}^{n} Q_i}{n} \; x \; t \; x \; \frac{P_a}{T_a} x \frac{298}{760} \tag{1}$$

Description:

V : the volume of air taken corrected under normal conditions of 25°C, 760 mmHg (m^3)
Qi : recording of i^{th} flowrate (m^3/min)
n : number of recorded flow rate
t : duration of test sampling (min)
P_a : average barometric pressure during sampling test (mmHg)
T_a : average temperature during test sampling in Kelvin (K)

Calculation of the concentration of pollutants in the ambient air

$$C = \frac{a}{v} \text{ x } 1000 \tag{2}$$

Description:
C : concentration of pollutants in the air ($\mu g/m^3$)
V : the volume of air taken corrected under normal conditions of 25°C,760 mmHg (m^3)
a : concentration of pollutants from the test sample based on the calibration curve ($\mu g/m^3$)
1000 : conversion of liters to m^3

Health Risk Assessment (HQ and HI)

To complement the concentration-based evaluation and assess potential non-carcinogenic health impacts, a quantitative health risk assessment was performed using the Hazard Quotient (HQ) and Hazard Index (HI). This framework follows the U.S. EPA methodology and recent applications in industrial and fertilizer-related air-pollution studies, as well as inhalation risk approaches commonly used in urban and industrial assessments (Abidin et al., 2024; Bhatta et al., 2025).

Exposure Concentration (EC)

Exposure concentration (EC, mg/m^3) was estimated by adjusting the measured ambient pollutant levels to represent long-term inhalation exposure, using the equation:

$$EC = \frac{C \times ET \times EF \times ED}{AT} \tag{3}$$

In this formulation, C refers to the measured concentration expressed in $\mu g/m^3$ and converted into mg/m^3, while ET represents the daily exposure duration of 8 hours. The EF parameter corresponds to an exposure frequency of 250 days per year, reflecting typical activity patterns for populations residing near industrial facilities. The ED, or exposure duration, was assigned a value of 30 years, a widely accepted assumption for chronic non-carcinogenic risk assessment in communities living near fertilizer factories and chemical-processing operations. The averaging time (AT) was calculated as the total number of hours across the entire exposure duration (ED × 365 × 24), ensuring that the resulting EC value reflects a realistic long-term exposure scenario. These exposure assumptions follow established risk-assessment protocols used in industrial air-pollution studies and have been consistently applied in recent environmental-health evaluations (Abidin et al., 2024; Bhatta et al., 2025).

Hazard Quotient (HQ)

The hazard quotient for each pollutant was calculated using:

$$HQ = \frac{EC}{RfC} \tag{4}$$

The reference concentrations (RfC) were selected based on established inhalation benchmarks: 0.04 mg/m^3 for NO_2, 0.02 mg/m^3 for SO_2, 0.50 mg/m^3 for NH_3, and 0.07 mg/m^3 for oxidants (expressed as ozone-equivalent exposure). These RfC values are consistent with toxicological thresholds commonly applied in multi-pollutant exposure assessments and have been used extensively in fertilizer-industry and combustion-related risk studies (Abidin et al., 2024; Bhatta et al., 2025). Incorporating these thresholds enables the HQ to quantify the extent to which the estimated exposure concentration approaches or exceeds established safe-exposure limits, thereby providing a robust basis for evaluating potential non-carcinogenic health risks.

Hazard Index (HI)

Cumulative non-carcinogenic risk from simultaneous exposure to multiple pollutants was evaluated using:

$$HI = \sum HQ_i \tag{5}$$

An HI > 1 indicates potential adverse health effects due to combined exposure, while HI < 1 suggests a low likelihood of non-carcinogenic impacts. Applying the HQ–HI framework provides a more comprehensive interpretation of pollutant exposure and is consistent with current analytical standards for industrial region air quality assessments (Abidin et al., 2024; Bhatta et al., 2025).

Results and Discussions

Assessment of ambient air for NO_2, SO_2, NH_3, and O_x

During sample collection, it is crucial to note the weather conditions at the sampling locations, as factors such as temperature, wind speed, wind direction, humidity, and air pressure can influence the test results for each ambient air gas parameter. Field data recording is presented in **Table 1**.

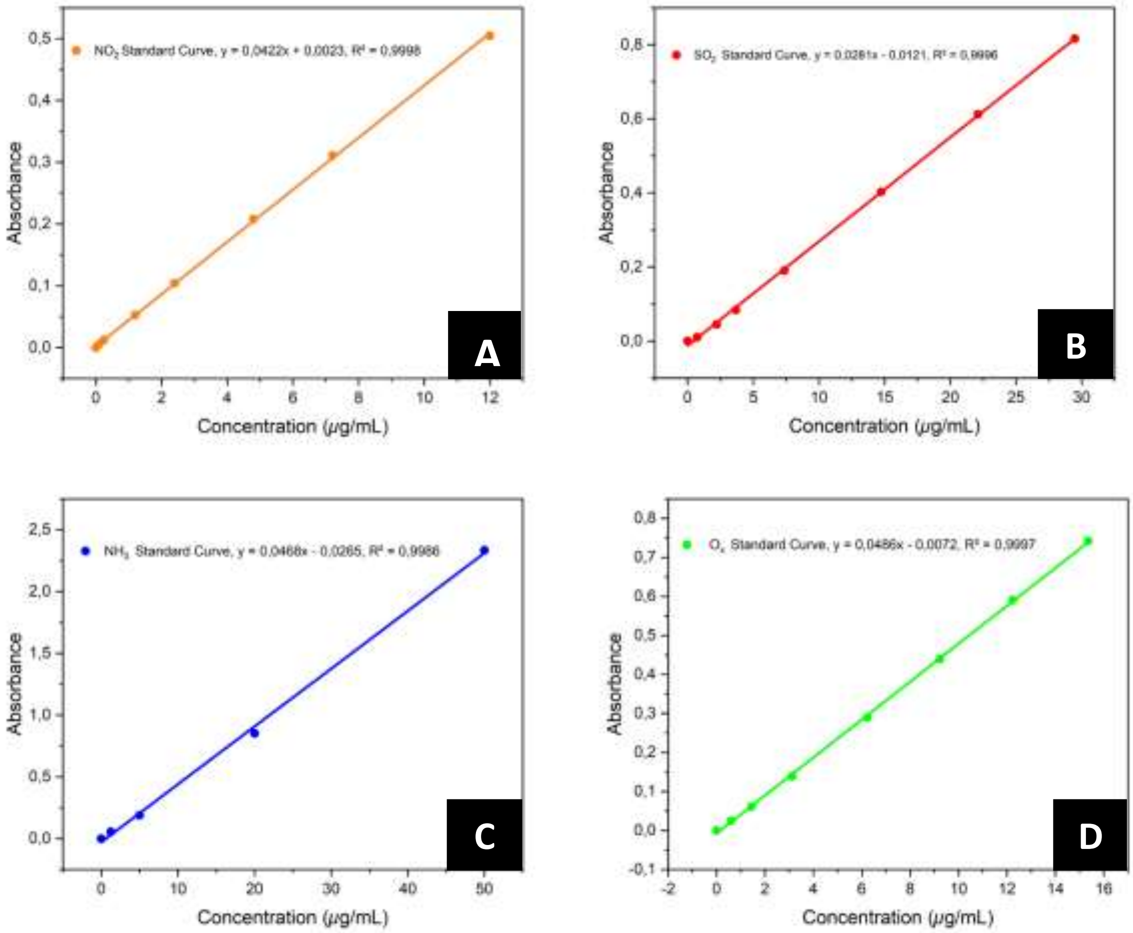

Figure 1. Standard Curve of (A) NO_2 with y = 0.0422x + 0.0023, R^2 = 0.9998, (B) SO_2 with y = 0.0281x – 0.0121, R^2 = 0.9996, (C) NH_3 with y = 0.0468x – 0.0265, R^2 = 0.9986, and (D) O_x with y = 0.0486x – 0.0072, R^2 = 0.9997

Table 1. Field state data of each sampling location

Point	Temperature (K)	Air pressure (mmHg)	Humidity (%)	Wind speed (m/s)	Wind Direction
A	306.95	755.0	66 - 80	0.9 – 2.2	West-East
B	305.95	758.0	64.6 – 65.2	1.3 – 2.0	West-East
C	307.15	756.7	63.4 – 63.9	0.9 – 2.1	West-East
D	309.4	758.9	62.33 – 63,00	2.2 – 2.44	West-East
E	308.5	758.2	62.2 – 62,4,4	0.9 – 2.1	West-East

By documenting these conditions, the impact of environmental factors on the test results can be assessed, ensuring the accuracy and reliability of the pollutant concentration measurements in the ambient air.

The sampling method using the InScienPro US-1012 impinger operates on the principle of drawing air through a pump and subsequently introducing it into each impinger tube, which contains absorbent solutions specific to each test parameter. The absorbent solutions react with airborne pollutants according to the parameters being tested. The sample's absorbance can then be measured, allowing the concentrations of the parameters in the sample to be determined using the standard curve shown in **Figure 1**. The concentrations of parameters in the test sample are presented in **Table 2**.

Table 2. The concentration of parameters in the air sample

Parameter	Point	Absorbance	Concentration (μg/mL)
NO_2	A	0.033	0.2535
	B	0.116	0.7274
	C	0.141	2.6943
	D	0.003	0.0360
	E	0.006	0.0965
SO_2	A	-0.0036	0.3024
	B	0.1503	5.7793
	C	0.0055	0.6263
	D	-0.0080	0.1459
	E	-0.0079	0.1472
NH_3	A	0.3301	7.6196
	B	0.2627	6.1794
	C	3.6011	77.5128
	D	0.1104	2.927
	E	0.1947	4.728
O_x	A	0.0330	0.7274
	B	0.1160	2.6943
	C	0.1410	3.2867
	D	-0.0067	0.0095
	E	-0.00401	0.0655

The concentration of parameters in the sample indicates the amount of pollutants absorbed in 10 mL of absorbent solution. However, to determine the concentration of pollutants in ambient air at the sampling location, it is necessary to know the volume of air sampled during the test, which can be calculated using **equation (1)**. Once the sampled air volume is known, the concentration of pollutant parameters in ambient air can be determined using **equation (2)**. The results of these calculations are presented in **Tables 3** and **4**.

Table 3. The concentration of NH_3 in Air

Parameters	Point	Volume of Air taken (m^3)	The concentration of C in the air (μg/mL)	Concentration (ppm)	Threshold value (ppm)
NH_3	A	69.44	109.72	0.1580	2
	B	69.94	88.34	0.1270	
	C	69.55	1114.46	1.6000	
	D	69.24	42.26	0.0607	
	E	69.38	68.14	0.0970	

Table 4. Concentration of NO_2, SO_2 and O_x in Air

Parameters	Point	Volume of Air Taken (m^3)	Concentration (μg/mL)	Threshold Value (μg/mL)
NO_2	A	23.14	12.57	200
	B	23.31	46.22	
	C	23.18	56.70	
	D	23.08	0.62	
	E	23.12	1.66	
SO_2	A	28.93	10.45	150
	B	29.14	198.30	
	C	28.97	21.61	
	D	28.85	5.05	
	E	28.91	5.09	
O_x	A	69.44	31.61	150
	B	69.94	9.32	
	C	69.55	15.73	
	D	34.62	0.13	
	E	34.69	0.94	

Risk analysis of NO_2

The concentration of NO_2 pollutants in ambient air can be determined using a UV-Vis spectrophotometer following the procedures outlined in SNI 7119-2:2017. Testing for NO_2 concentration begins with sampling using Griess Saltzman absorbent media. NO_2 pollutants, existing as gases with pH 2.0 – 2.5, react with Griess Saltzman reagent to form a pink azo dye. The azo compound formed from NO_2 gas in the sample reacts and converts to HNO_3, which then reacts with an amine compound. Additionally, protonation reactions occur in oxygen and nitrosamine compounds by acetic acid and free protons in the sample solution. The resulting chemical structure removes water molecules to form a diazonium ion, as shown in the proposed mechanism reaction in **equations (6)**, **(7)**, and **(8).**

$$2NO_2(g) + H_2O\ (aq) \longrightarrow HNO_2\ (aq) + NO_3^-\ (aq) \tag{6}$$

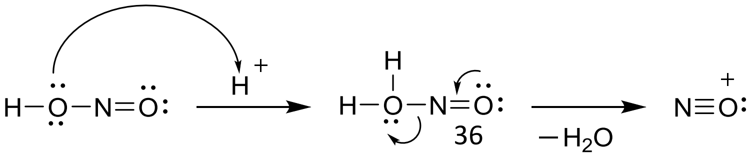

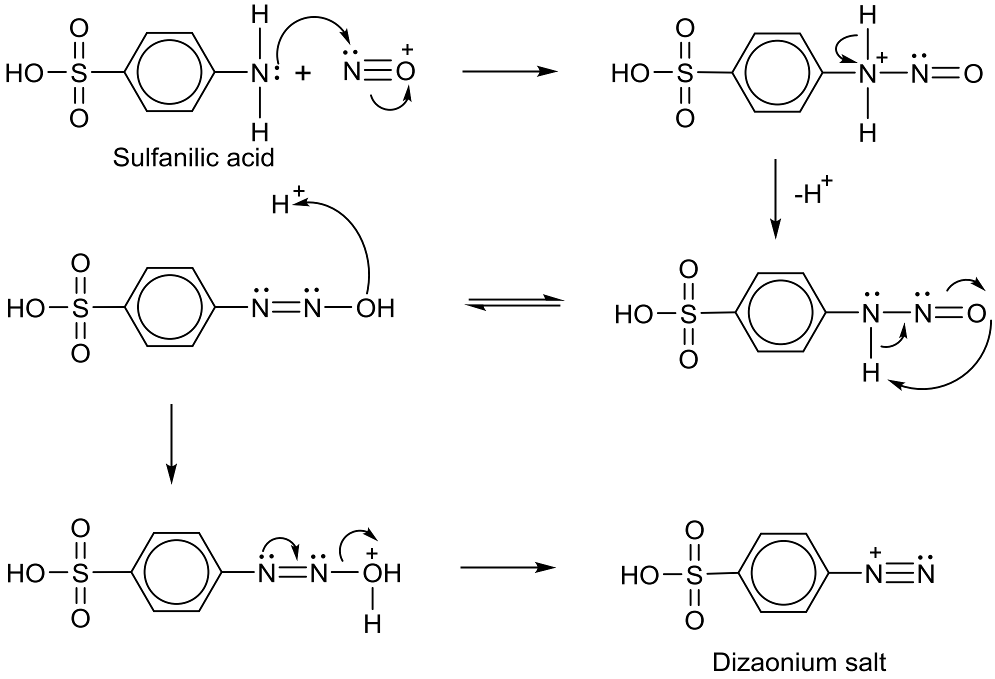

(7)

(8)

Ion diazonium is an electrophilic ion that reacts with *N*-(1-naphthyl ethylenediamine dihydrochloride) Eriodictyol (N-NED) and forms an azo compound (-N=N) that exhibits a pink colour. The concentration of NO_2 correlates directly with the intensity of the sample's colour; the darker the sample, the higher its concentration. The concentration of NO_2 is calculated using the Beer-Lambert law, and the linear regression equation is derived from the standard solution curve shown in **Figure 2**. Ambient air samples of NO_2 were taken from three points around a fertilizer industry plant. The collected NO_2 samples were analyzed directly as solutions, with absorbance readings taken using a UV-Vis spectrophotometer at a maximum wavelength of 550 nm. The data from the NO_2 concentration analysis in the samples are presented in **Table 2**.

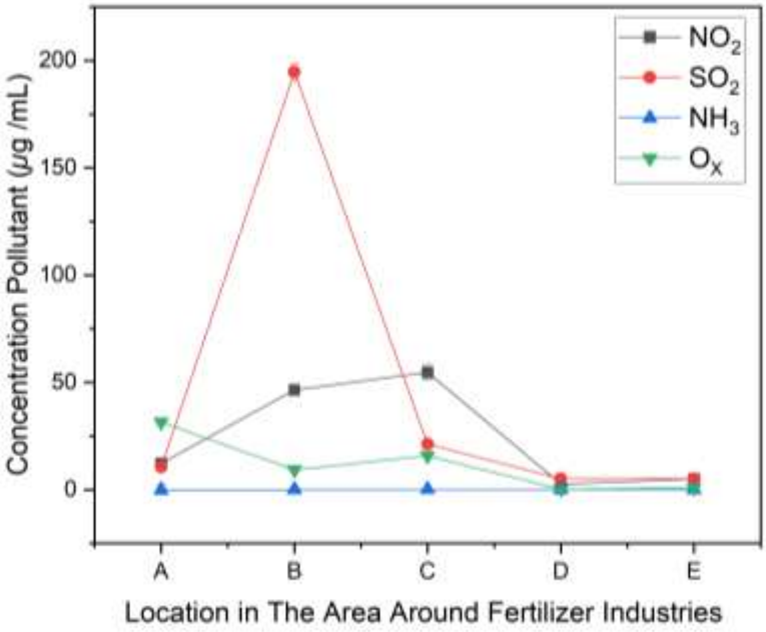

Figure 2. Annual Average Analysis of Pollutant Monitoring at Fertilizer Factories in Indonesia: Concentrations of NO_2, SO_2, and O_x in μg/mL, and NH_3 in ppm at Various Monitoring Points (Point A: Industrial Fertilizer Product Storage Warehouse, Point B: Office Area, Point C: Inside Fertilizer Processing Plant, Point D: Entrance Gate of Industrial Area, Point E: Surrounding Village)

Various production machines rely on fuel combustion the fertilizer production process. These machines can emit pollutants from fossil fuel combustion (Liu et al., 2023; Tang et al., 2020; Shi et al., 2024). One such pollutant is NO_2, a byproduct of incomplete combustion. Production machines must have adequate exhaust systems to properly vent gases without harming nearby individuals (Xiao et al., 2023). Prolonged exposure to NO_2 concentrations above threshold levels poses health risks, including Chronic Obstructive Pulmonary Disease (COPD) (Liu et al., 2023; Luo et al., 2016). Additionally, NO_2 is implicated in the formation of other air pollutants, such as $PM_{2.5,}$ by directly contributing to the production of nitrate compounds (Chu et al., 2020).

The data from testing in **Table 4** shows that NO_2 concentrations in ambient air around the fertilizer industry comply with quality standards set by the Republic of Indonesia Government Regulation No. 22/2021 on Environmental Protection and Management. Each sampling point indicates NO_2 concentrations below the permissible 200 μg/Nm^3 limit. **Table 4** reveals a trend where concentrations increase from points A to C, which sequentially approach the main production area of the fertilizer industry. Specifically, point A is a residential area near the industry, point B is within the industry's office area, and point C is within the production zone. Concentrations rise from sample point A to C due to their proximity to the fertilizer production facilities, where NO_2 emissions from vehicle engines, power generation, and industrial activities are prevalent. Sample point C, closest to the fertilizer production area, shows the highest NO_2 concentration at 56.7070 μg/Nm^3.

In contrast, points D and E exhibit significantly lower NO_2 concentrations as they are farther from the industrial site. None of the five samples exceed the threshold limit for NO_2 concentrations, ensuring no immediate health risks to humans or the surrounding environment.

Risk analysis of SO_2

The concentration testing of SO_2 begins with sampling using tetrachloromercurate(II) (TCM) absorbent media. A complex compound, dichlorosulfonylmercurate, forms when TCM absorbs SO_2 pollutants. The reaction proceeds as follows:

$$2HgCl_4^{2-}(aq) + 2SO_2(g) + 2H_2O(l) \longrightarrow 2HgCl_4SO_3^{2-}(aq) + 4H^+(aq) \qquad (9)$$

$$HCHO(aq) + SO_2(aq) + H_2O(l) \longrightarrow HOCH_2SO_3H(aq) \qquad (10)$$

Before the absorbance reading was done using a spectrophotometer, the obtained sample was first reacted with a solution of sulfamic acid. Sulfamic acid removes interfering ions. Next, the sample is reacted with formaldehyde to preserve its stability, as SO_2 solutions are prone to volatilization upon exposure to light due to photolysis reactions. It must have a visible colour to ensure the sample can be read using a UV-Vis spectrophotometer. Therefore, pararosaniline is added to form a complex compound known as pararosaniline methyl sulfonate, which is purple in colour and easily visible. The concentration of SO_2 is calculated using the Lambert-Beer law. After sample preparation, absorbance is measured using a UV-Vis spectrophotometer at a wavelength of 550 nm. The data from the analysis of SO_2 concentration in the samples are presented in **Table 2**.

The source of SO_2 emissions from fertilizer plants originates not directly from the fertilizer processing but from the boilers used within these plants. In fertilizer plants, boilers typically use fossil fuels such as coal or petroleum to supply the necessary energy for production. When these fuels are burned, sulfur oxidation reactions occur, resulting in the emission of SO_2 gas (Hu et al., 2024). SO_2 gas is colourless but has a pungent odour. It is also a pollutant that contributes to smog formation, often found in densely populated urban areas. Furthermore, when SO_2 gas reacts with atmospheric water vapour, it forms H_2SO_4, which then condenses and falls to the ground as acid rain, capable of damaging buildings, vegetation, and other materials.

In addition to its environmental impacts, SO_2 pollution has adverse health effects on individuals exposed to it (Zhang et al., 2020). These health effects include respiratory tract irritation and reduced lung function manifested by symptoms such as shortness of breath, increased asthma incidents, and coughing. According to material safety data sheets, SO_2 exposure can also cause throat and sinus irritation, eye irritation, lung edema, and, in severe cases, fatalities.

The results from **Table 4** show that the concentration of SO_2 in ambient air around the fertilizer plant, according to Indonesian Government Regulation No. 22 of 2021 on Environmental Protection and Management, indicates that sampling points A, C, D, and E have SO_2 concentrations below the permissible limit of 150 $\mu g/m^3$. However, sampling point B exceeds this limit, showing a high concentration of 198.3065 $\mu g/m^3$. This higher concentration at point B is due to its proximity to the coal-fired boiler in the fertilizer plant, which is a primary source of SO_2 emissions. The presence of the boiler significantly affects the air quality near the fertilizer plant, resulting in elevated SO_2 concentrations.

Reducing SO_2 emissions from industrial boilers can be achieved through various strategies and technologies. Switching to low-sulfur fuels like natural gas or cleaner fuels can significantly reduce SO_2 emissions. Installing Flue Gas Desulfurization (FGD) systems is a standard method to control SO_2 emissions by removing sulfur dioxide from exhaust gases before they are released into the atmosphere. Improving boiler performance efficiency can reduce fuel consumption and lower SO_2 emissions. Regular maintenance and optimal operation of boilers help maintain efficient performance and reduce the likelihood of high SO_2 emissions. Effective reduction of SO_2 emissions from industrial boilers often requires combining these strategies based on operational needs.

Risk analysis of NH_3

The determination of ammonia concentration is conducted using the indophenol method, with the sample's absorbance read using a UV-Vis spectrophotometer. Airborne pollutant samples are collected through an absorbing solution of sulfuric acid (H_2SO_4), where the NH_3 sample and the absorbing solution form ammonium sulfate. The reaction that occurs is as follows:

$$2NH_3(g) + H_2SO_4(aq) \longrightarrow (NH_4)_2SO_4(aq) \tag{11}$$

Maintaining the correct pH is essential in the indophenol method for determining ammonia concentration. The pH level must range between 8 and 11.5 to ensure the proper formation of indophenol. If the pH exceeds 11.5, ammonia may only partially convert to nitrite, resulting in undetectable blank concentrations. Conversely, if the absorbing solution is too acidic, with a pH below 8, the method will lack sensitivity entirely (Lewandowska & Falkowska, 2004). The proposed mechanism reaction for the formation of indophenol is shown in equation **(12)**, **(13)**, and **(14)**.

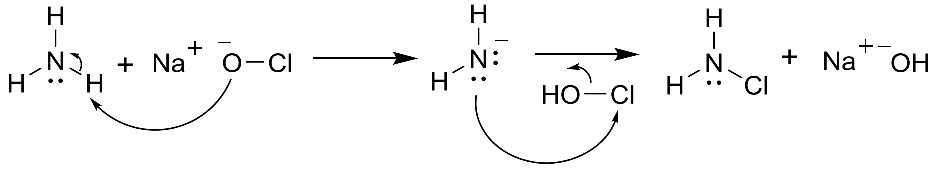

(12)

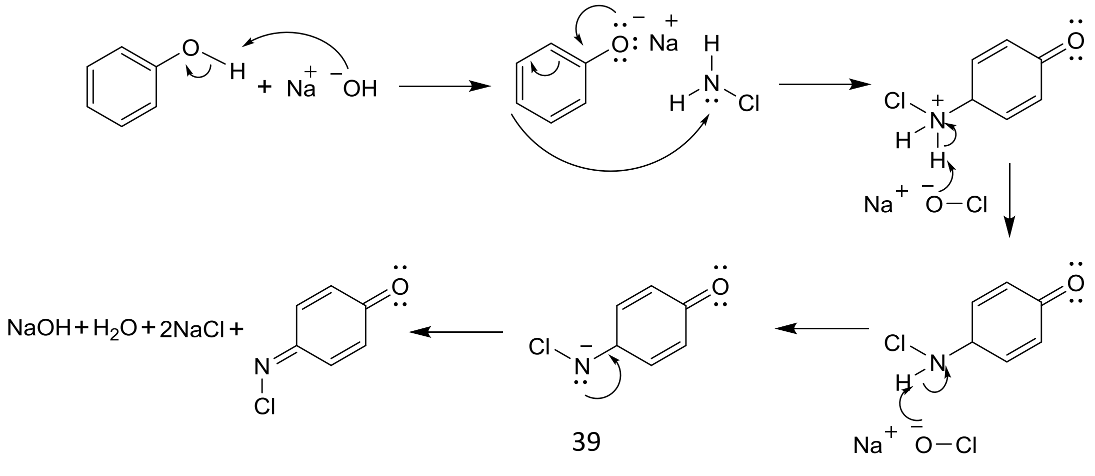

(13)

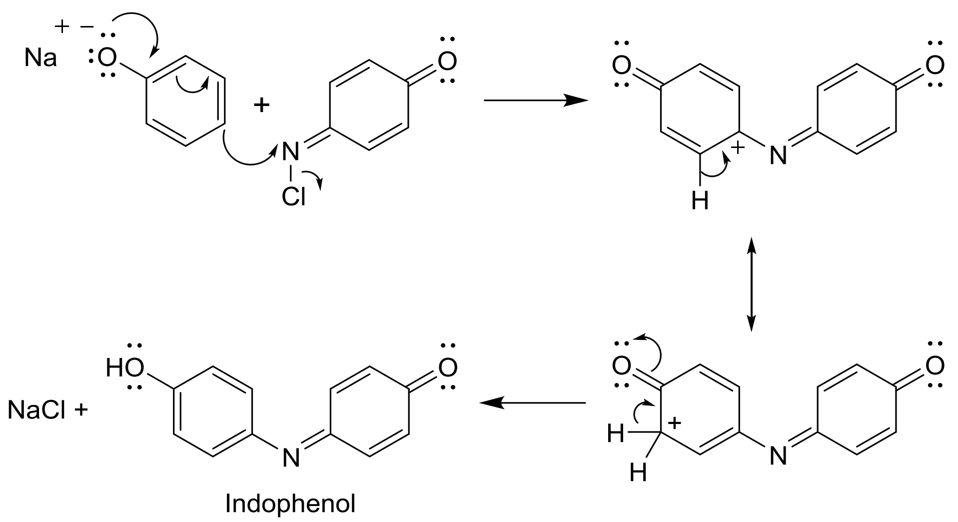

(14)

Under alkaline conditions, phenol and sodium hypochlorite react with the sample solution to form a blue indophenol complex. Sodium nitroprusside is used as a catalyst in the test to expedite the reaction. A spectrophotometer measures the intensity of the blue colour at 630 nm in the visible spectrum (SNI 7119-7:2017).

Ambient air samples containing NH_3 gas were collected around the fertilizer plant from three locations. The NH_3 samples obtained were in solution form and immediately analyzed by measuring absorbance using a UV-Vis spectrophotometer at 630 nm. The results of the NH_3 concentration analysis in the samples are presented in **Table 2**.

NH_3 is a product of protein decomposition by microbes in compost waste (Nordahl et al., 2023) and is a major atmospheric pollutant that significantly impacts air acidity (Coelho et al., 2010). NH_3 plays a crucial role in fertilizer production. The primary source of NH_3 from fertilizer plants is the production of ammonia-based fertilizers such as ammonium nitrate (NH_4NO_3) and urea ($CO(NH_2)_2$). The production of ammonia-based fertilizers, like ammonium nitrate and urea, involves the synthesis of NH_3 as a part of the manufacturing process. The primary source of NH_3 in fertilizer production is the Haber-Bosch process, a chemical reaction combining nitrogen gas (N_2) from the air with hydrogen gas (H_2) derived from natural gas. The produced ammonia is used as the main ingredient in various nitrogen-based fertilizers. During the production of ammonia-based fertilizers, some ammonia may also be released into the atmosphere as emissions due to inefficient production processes. These emissions can contribute to elevated ammonia levels in the atmosphere, particularly around fertilizer plants. NH_3 is an essential component of fertilizers because it provides plants with nitrogen, which is crucial for their growth. However, excessive NH_3 emissions from fertilizer plants or agricultural activities can have environmental implications, such as contributing to air pollution and the formation of delicate particulate matter ($PM_{2.5}$) (Bachmann et al., 2015; Lunghi et al., 2024). NH_3 also has adverse health effects on humans, such as irritating the eyes, respiratory system, and skin. NH_3 has a very pungent odour, which can disrupt environmental quality (Yan et al., 2024).

The data in **Table 3** show that the NH_3 concentration in the ambient air of the fertilizer industry, based on the standard quality according to the Decree of the State Minister for the Environment No. 50 of 1996 concerning Odor Level Standards, indicates that all testing points still have NH3 concentrations in the air below the standard limit of 2 ppm. Testing points B, D, and E have low NH_3 concentration values in the air, which can be attributed to points B, D, and E being relatively far from fertilizer materials. It is known that the decomposition of organic matter, especially animal waste, which is a primary component of fertilizers, is a significant contributor to NH_3 gas. Therefore, the closer the testing points are to the fertilizer materials, such as points A and C, the higher the NH_3 concentration in the air, with sample C showing a relatively high value of 1.6 ppm.

Reducing NH_3 emissions from fertilizer plants can be achieved through several measures, such as installing ammonia recovery systems to capture and recycle NH_3 emissions during fertilizer production. This step can help reduce ammonia emissions and improve the overall efficiency of the production process. Maintaining aerobic conditions is crucial for controlling NH_3 and other odorous emissions because many of these compounds are produced through anaerobic processes (Andraskar et al., 2021). Implementing emission monitoring systems to track NH_3 emissions is also important. Regular emission monitoring can help identify areas for improvement and ensure compliance with environmental regulations. Additionally, educating farmers and the community about proper fertilizer use and its environmental impact can support efforts to minimize NH_3 emissions across the entire fertilizer use chain.

Risk analysis of O_x

Determining oxidant (O_x) concentration was carried out using a UV-Vis spectrophotometer. Air samples were collected using a neutral buffer potassium iodide (NBKI) absorbing solution. The principle of analyzing oxidant gases using UV-Vis spectrophotometry involves oxidants from ambient air being absorbed by the NBKI solution and reacting with iodide ions, thereby releasing iodine (I_2), which is pale yellow. The concentration of the solution is determined spectrophotometrically at a wavelength of 350.1 nm. The reaction that occurs is as follows:

$$O_3(g) + 2KI(aq) \longrightarrow K_2O(aq) + I_2(g) + O_2(g) \tag{15}$$

The standard curve was created using a certified reference material (CRM) iodine stock solution of known concentration. Ambient air samples of oxidant gas (O_x) were collected from three points around the fertilizer industry factory. The collected O_x samples, in solution form, were immediately analyzed by measuring absorbance using a UV-Vis spectrophotometer at a wavelength of 350 nm. After obtaining the absorbance values, the concentration of O_x in the samples was determined using Lambert-Beer's law with the above linear regression equation. The data from the analysis of Ox concentration in the samples are presented in **Table 2**.

Oxidants act as oxidizers, meaning they do not undergo oxidation by oxygen and thus produce secondary pollutants. Oxidant air pollutants in the atmosphere originate from photochemical reactions involving hydrocarbons, which form ozone, peroxyacetyl nitrate (PAN), and NO_2. Ozone is a colourless gas at room temperature that condenses to form a blue liquid at -111°C and freezes into a dark blue solid at -192°C. Ozone is a highly reactive and easily reducible gas, blue in colour, and capable of severely irritating the respiratory system. It can be detected by the human nose at concentrations as low as 0.001 ppm (parts per million). The maximum allowable ozone concentration in ambient air is about 0.01 ppm; however, concentrations up to 1.00 ppm are considered safe if exposure does not exceed 10 minutes.

The test results in **Table 4** indicate that the O_x concentration in the ambient air surrounding the fertilizer industry is below the standard threshold of 150 $\mu g/m^3$, as stipulated in Indonesian Government Regulation Number 22 of 2021 on Environmental Protection and Management. Among the five samples, sample A had the highest O_x concentration at 31.6461 $\mu g/m^3$.

Integrated Spatial Risk Assessment Using Hazard Quotient (HQ) and Hazard Index (HI)

The spatial assessment of non-carcinogenic risks based on HQ–HI reveals pronounced heterogeneity in pollutant exposure across the fertilizer industrial area. **Table 5** presents HQ values for NO_2, SO_2, NH_3, and oxidants (Ox), alongside the cumulative HI at each location. These patterns reflect the interplay between industrial processes, emission sources, and atmospheric dispersion around the fertilizer complex.

Table 5. Hazard Quotient (HQ) and Hazard Index (HI) across all sampling points

Pollutant	Point A	Point B	Point C	Point D	Point E
HQ–NO_2	0.034	0.126	0.154	0.002	0.004
HQ–SO_2	0.014	0.794	0.087	0.020	0.021
HQ–NH_3	0.220	0.177	2.238	0.085	0.137
HQ–Ox	0.263	0.078	0.131	0.001	0.007
HI (ΣHQ)	0.53	**1.17**	**2.61**	0.11	0.17

The risk pattern is strongly driven by SO_2 at Point B and NH_3 at Point C, both of which represent characteristic emissions of fertilizer-related industrial operations. Point B showed the highest HQ–SO_2 (0.794), indicating substantial influence from combustion sources, including boiler activities and fuel-based operations. Similar sulfur-driven risk profiles have been reported in industrial emission zones in Asia and South America, where combustion processes are dominant contributors to HI (Ramírez et al., 2025).

Point C exhibited notably high HQ–NH_3 (2.238) and elevated HQ–NO_2 (0.154), consistent with emissions from nitrogen-based fertilizer synthesis, ammonia handling, and volatilization processes. Comparable NH_3- and NO_2-driven risks have been identified in agrochemical and fertilizer corridors in China, India, Indonesia, and Morocco (Ababio et al., 2025), reinforcing the relevance of these pollutants as key drivers in industrial nitrogen-processing environments.

Oxidant (Ox) exposure contributed minimally to cumulative risks. However, it displayed a moderate HQ–Ox (0.263) at Point A, which may reflect localized photochemical reactivity involving NO_x and reactive organic compounds near the facility perimeter. This behavior is consistent with oxidant formation patterns observed in fertilizer-associated industrial corridors (Bhatta et al., 2025).

Table 6. Comparison of International Air-Pollution Risk Assessments

Study	Setting	Key Pollutants	*Risk Metrics	Key Findings	Relevance to Present Study
Present study (2025)	Fertilizer industrial zone, Indonesia	NO_2, SO_2, NH_3, Ox	HQ, HI	Localized risk at Points B & C; NH_3 & SO_2 dominant	Baseline HQ–HI for fertilizer gas-phase emissions
Abidin et al., 2024	Indonesia	$PM_{2.5}$	RQ	RQ > 1; respiratory links	Complements gas-phase risks with particulate-based risk evidence
Bhatta et al., 2025	Thailand	$PM_{2.5}$, PM_{10}	HQ, HI, AQI	Seasonal HI up to 9	Illustrates cumulative risk escalation in dense urban zones
Ababio et al., 2024	Ghana	$PM_{2.5}$, NO_2, O_3	HQ, HI, DD, AQLI	HQ/HI elevated nationally; O_3 impacts significant	Provides oxidant (O_3) risk comparison relevant to Ox
Lee et al., 2024	South Korea	PAHs, metals	CARI	Metals dominate toxicity-weighted risk	Parallel to use of integrated risk metrics
Ramírez et al., 2025	Latin America	PM_{10} + metals; fertilizer contrib. ~3%	HQ, HI, cancer risk	Metal risks high despite low PM mass	Mirrors pollutant-specific drivers (NH_3, SO_2) dominating risk

*Note:

HQ	: Hazard Quotient (Ratio of exposure concentration (EC) to reference concentration (RfC) for individual pollutants).
HI	: Hazard Index (Sum of HQ values across pollutants; HI > 1 indicates potential non-carcinogenic risk).
RQ	: Risk Quotient (Similar to HQ but used primarily for particulate matter).
DD	: Daily Dose (Dose estimation used in chronic exposure models).
AQLI	: Air Quality Life Index (Converts chronic PM exposure into estimated life-expectancy loss).
CARI	: Comprehensive Air-Risk Index (Toxicity-weighted multi-pollutant risk index, used in industrial PM studies).

The cumulative hazard index underscores these differences. HI exceeded 1 at Point B (HI = 1.17) and Point C (HI = 2.61), indicating potential chronic non-carcinogenic health risks from combined pollutant exposure. By contrast, Points A, D, and E exhibited HI values well below threshold levels, suggesting effective dilution and reduced emission influence with increasing distance from core industrial operations. Similar attenuation gradients have been documented in fertilizer-production regions of Southeast Asia and peri-urban industrial settings in Latin America (Abidin et al., 2024; Ramírez et al., 2025).

Taken together, the HQ–HI framework provides a risk-oriented interpretation of pollutant concentrations by contextualizing the measured values into health-relevant indicators. This spatially resolved assessment offers a clearer understanding of the cumulative risk profile and demonstrates that NH_3 and SO_2 exert relatively higher contributions to the overall risk pattern in areas influenced by fertilizer-industry activities.

To further contextualize these results, **Table 6** compares the present findings with international studies assessing non-carcinogenic risks in industrial, urban, and fertilizer-related settings.

Overall, the integrated spatial risk assessment demonstrates that the fertilizer industrial area exhibits distinct pollutant-driven risk zones, with NH_3 and SO_2 emerging as the principal contributors to non-carcinogenic exposure burdens. These findings align closely with international evidence from fertilizer-production regions and combustion-intensive industrial environments. The coherence between local and global patterns underscores the necessity of risk-based approaches, such as HQ–HI to complement concentration-based assessments and inform appropriate mitigation strategies.

Conclusion

The ambient air quality in and around the fertilizer industry was evaluated by analyzing four key gaseous pollutants, which include NO_2, SO_2, NH_3, and oxidants (O_x). Their potential non-carcinogenic health impacts were assessed using the Hazard Quotient (HQ) and Hazard Index (HI). The measured concentrations were compared with Indonesian regulatory thresholds, with limits of 200 $\mu g/m^3$ for NO_2, 150 $\mu g/m^3$ for SO_2, 2 ppm for NH_3, and 150 $\mu g/m^3$ for oxidants. Most measured concentrations remained below their respective threshold limits, except for SO_2 at Point B and NH_3 at Point C, which showed elevated levels consistent with combustion activities and fertilizer-processing operations. These findings were further supported by the risk assessment, which showed that HQ values for SO_2 at Point B (HQ = 0.794) and NH_3 at Point C (HQ = 2.238) were the dominant contributors to cumulative exposure. The Hazard Index exceeded the non-carcinogenic risk threshold (HI > 1) at Point B (HI = 1.17) and Point C (HI = 2.61), indicating potential long-term health concerns in areas closest to emission sources. In contrast, Points A, D, and E demonstrated low risk, reflecting effective atmospheric dispersion with increasing distance from industrial activities. Overall, the integrated concentration-based and risk-based evaluation shows that the fertilizer production zone exhibits localized pollutant and risk intensification, particularly for SO_2 and NH_3. These results underscore the need for improved emission control, optimized combustion practices, and strengthened monitoring strategies to minimize exposure for workers and surrounding communities.

Acknowledgments

No external assistance or contributions beyond our regular duties were involved in this research. We, the authors, take full responsibility for the content, interpretations, and any errors or omissions in this work.

Conflicts of interest

The authors declare that there are no conflicts of interest.

References

Ababio, B. A., Ashong, G. W., Agyekum, T. P., Yeboah, B. A., Nkansah, M. A., Hogarh, J. N., Commeh, M. K., Kwaansa-Ansah, E. E., Dabie, K., Adulley, F., Boansi, E., Sarbeng, L., Adu Ababio, B., Boapea, M. S., Oduro Darko, N. K., & Appiah, M. K. (2024). Comprehensive health risk assessment of urban ambient air pollution ($PM_{2.5}$, NO_2 and O_3) in Ghana. *Ecotoxicology & Environmental Safety*, *298*, 117591. https://doi.org/10.1016/j.ecoenv.2024.117591.

Abidin, Z. U., Maziya, F. B., Susetyo, S. H., Yoneda, M., & Matsui, Y. (2024). Heavy metal air pollution in an Indonesian landfill site: Characterization, sources, and health risk assessment for informal workers. *Environmental Advances*, *8*, 100512. https://doi.org/10.1016/j.envadv.2024.100512.

Alighiri, D., Wardani, S., & Harjito. (2015). Sintesis selulosa asetat dari jerami padi sebagai upaya penanggulangan limbah pertanian. In *Proceeding Seminar Nasional Kimia dan Pendidikan Kimia SNKPK* (p. 28).

Arshad, M., & Shanavas, P. (2013). Comparison of serum and urinary fluoride levels among fertilizer and wood industry workers in Mangalore city, India. *Fluoride, 46*(2), 80-82.

Bellouin, N., Quaas, J., Gryspeerdt, E., Kinne, S., Stier, P., Watson-Parris, D., & Stevens, B. (2020). Bounding global aerosol radiative forcing of climate change. *Reviews of Geophysics, 58*(1).

Bhatta, J., Laosee, O., Janmaimool, P., Strezov, V., & Rattanapan, C. (2025). Spatiotemporal analysis of particulate matter (PM_{10} and $PM_{2.5}$) and health risks in Thailand's urban core. *Chemosphere*, *344*, 144687. https://doi.org/10.1016/j.chemosphere.2025.144687.

Bocato, M. Z., Sanches, D., Vaz, B. G., Pereira, M., Tavares, D. S., & Gobo, G. (2019). An overview of the current progress, challenges, and prospects of human biomonitoring and exposome studies. *Journal of Toxicology and Environmental Health, Part A, 82*(5-6), 131-156.

Bowden, D. J., & Brimblecombe, P. (2003). The rate of metal catalyzed oxidation of sulfur dioxide in collagen surrogates. *Journal of Cultural Heritage, 4*(2), 137-147.

Cai, N., Zhao, Y., Xu, F., Jiang, M., Han, L., Zhu, B., & Wang, B. (2025). Integrated internal and external exposure models for dimethylformamide risk assessment and health risk monetization. Ecotoxicology & Environmental Safety, 291, 117890. https://doi.org/10.1016/j.ecoenv.2025.117890.

Chheang, L., Heng, S., Neth, P., Sin, S., Kimhong, S., & Lay, K. S. (2021). Heavy metal contamination and human health implications in the Chhne Tnal reservoir, Cambodia. *Sustainability, 13*(24), 13538.

Chu, B., Ma, Q., Liu, J., Ma, J., Zhang, P., Chen, T., Feng, Q., Wang, C., Yang, N., Ma, H., Russell, A. G., & He, H. (2020). Air pollutant correlations in China: Secondary air pollutant responses to NO_x and SO_2 control. *Environmental Science & Technology Letters, 7*(10), 695-700. https://doi.org/10.1021/acs.estlett.0c00403.

Coelho, L. H. G., Melchert, W. R., Rocha, F. R., Rocha, F. R. P., & Gutz, I. G. R. (2010). Versatile microanalytical system with porous polypropylene capillary membrane for calibration gas generation and trace gaseous pollutants sampling applied to the analysis of formaldehyde, formic acid, acetic acid and ammonia in outdoor air. *Talanta, 83*(1), 84-92. https://doi.org/10.1016/j.talanta.2010.08.045.

Fowler, B. A., Yamauchi, H., Conner, E. A., & Akkerman, M. (1993). Cancer risks for humans from exposure to the semiconductor metals. *Scandinavian Journal of Work, Environment & Health, 1*, 101-103.

Ghavam, S., Vahdati, M., Wilson, I. A. G., & Styring, P. (2021). Sustainable ammonia production processes. *Frontiers in Energy Research, 9*, 580808. https://doi.org/10.3389/fenrg.2021.580808.

Gong, C., Xin, J., Wang, S., Wang, Y., & Zhang, T. (2017). Anthropogenic aerosol optical and radiative properties in the typical urban/suburban regions in China. *Atmospheric Research, 197*, 177-187.

Hong, Z., Wang, Z., & Li, X. (2017). Catalytic oxidation of nitric oxide (NO) over different catalysts: An overview. *Catalysis Science & Technology, 7*(16), 3440-3452.

Ji, X., Han, M., Yun, Y., Li, G., & Sang, N. (2015). Acute nitrogen dioxide (NO_2) exposure enhances airway inflammation via modulating Th1/Th2 differentiation and activating JAK-STAT pathway. *Chemosphere, 120*, 722-728.

Kalbarczyk, R., Ziemiańska, M., Nierbca, A., & Dobrzańska, J. (2018). The impact of climate change and strong anthropopressure on the annual growth of Scots pine (Pinus sylvestris L.) wood growing in eastern Poland. *Forests, 9*(11), 661. https://doi.org/10.3390/f9110661.

Kelly, F. J., & Fussell, J. C. (2015). Air pollution and public health: Emerging hazards and improved understanding of risk. *Environmental Geochemistry and Health, 37*(4), 631-649.

Kuzmanović, P., Knežević, D., Milenković, B., Vukanac, I., Marković, T., & Rajšić, S. (2022). Radioactivity of fertilizers used in Serbia and dose assessments for workers in the industry. *Journal of Radioanalytical and Nuclear Chemistry*, 1-10.

Larsen, R. (2000). Experiments and observations in the study of environmental impact on historical vegetable tanned leathers. *Thermochimica Acta, 365*(1), 85-99.

Lee, E. K., Romeiko, X. X., Zhang, W., Feingold, B. J., Khwaja, H. A., Zhang, X., & Lin, S. (2021). Residential proximity to biorefinery sources of air pollution and respiratory diseases in New York State. *Environmental Science & Technology, 55*(14), 10035-10045. https://doi.org/10.1021/acs.est.1c00698.

Lee, S.-J., Cho, I.-G., Lee, H.-Y., Ju, J.-T., Shin, H.-J., & Choi, S.-D. (2024). Development of a comprehensive air risk index and its application to high spatial-temporal health risk assessment in a large industrial city. Environmental Pollution, 335, 125545. https://doi.org/10.1016/j.envpol.2024.125545.

Liu, C., Chen, R., Lei, J., Zhu, Y., Zhou, L., Meng, X., Xuan, J., & Kan, H. (2023). Ambient nitrogen dioxide and hospitalizations of full-spectrum respiratory diseases: A national case-crossover study. *Environmental Health, 1*(2), 130-138. https://doi.org/10.1021/envhealth.3c00039.

Liu, S., Xing, J., Zhao, B., Wang, J., Wang, S., Zhang, X., & Ding, A. (2019). Understanding of aerosol–climate interactions in China: Aerosol impacts on solar radiation, temperature, cloud, and precipitation and its changes under future climate and emission scenarios. *Current Pollution Reports, 5*(1), 36-51.

Luo, K., Li, R., Li, W., Wang, Z., Ma, X., Zhang, R., Fang, X., Wu, Z., Cao, Y., & Xu, Q. (2016). Acute effects of nitrogen dioxide on cardiovascular mortality in Beijing: An exploration of spatial heterogeneity and the district-specific predictors. *Scientific Reports*. https://doi.org/10.1038/srep38328.

Nordahl, S. L., Preble, C. V., Kirchstetter, T. W., & Scown, C. D. (2023). Greenhouse gas and air pollutant emissions from composting. *Environmental Science & Technology, 57*(6), 2235-2247. https://doi.org/10.1021/acs.est.2c05846.

Priatmoko, S., Alighiri, D., Drastisianti, A., Harjunowibowo, D., Nur Rohman, A., & Sulistyaningsih, T. (2024). Coagulant preparation from glutaraldehyde-crosslinked durian skin cellulose for treatment of wastewater generated by sugar palm starch industries. *Cellulose Chemistry and Technology, 58*(1-2), 201-214.

Ramírez, O., Gutiérrez-Ulloa, C., Zárate, L., Carrión, A. M., Hernández Guzmán, A., & de la Rosa, J. (2025). Impact of urbanization and industrialization on PM_{10} in municipalities near megacities: A case study from an Andean region, Latin America. Urban Climate, 45, 102612. https://doi.org/10.1016/j.uclim.2025.102612.

Salmon, L. G., Cass, G. R., Bruckman, K., & Haber, J. (2000). Ozone exposure inside museums in the historic central district of Krakow, Poland. *Atmospheric Environment, 34*(23), 3823-3832.

Sarudji, D. (2010). *Environmental health*. Karya Putra Darwati.

Shah, A. S. V., Lee, K. K., McAllister, D. A., Hunter, A., Nair, H., Whiteley, W., Langrish, J. P., Mills, N. L., & Newby, D. E. (2015). Short term exposure to air pollution and stroke: Systematic review and meta-analysis. *BMJ, 350*, h1295.

SNI. (2017). Ambient air - Part 1: Determination of ammonia (NH_3) content using an indophenol spectrophotometer (SNI 19-7119.1-2017). Jakarta: Badan Standardisasi Nasional.

SNI. (2017). Ambient air - Part 2: Determination of nitrogen dioxide (NO_2) content by Griess-Saltzman method using spectrophotometer (SNI 7119-2:2017). Jakarta: Badan Standardisasi Nasional.

SNI. (2017). Ambient air - Part 7: Determination of sulfur dioxide (SO_2) content by pararosaniline method using spectrophotometer (SNI 7119-7:2017). Jakarta: Badan Standardisasi Nasional.

SNI. (2017). Ambient air - Part 8: Determination of oxidants by neutral buffer potassium iodide (NBKI) method using spectrophotometer (SNI 7119-8:2017). Jakarta: Badan Standardisasi Nasional.

Tang, R., Zhao, J., Liu, Y., Huang, X., Zhang, Y., Zhou, D., Ding, A., Nielsen, C. P., & Wang, H. (2022). Air quality and health co-benefits of China's carbon dioxide emissions peaking before 2030. *Nature Communications, 13*(1). https://doi.org/10.1038/s41467-022-28672-3

Vallero, D. (2008). *Fundamentals of air pollution* (4th ed.). Academic Press.

Walford, H. H., & Doherty, T. A. (2013). STAT6 and lung inflammation. *Jak-Stat, 2*.

WHO. (2018). Ambient (outdoor) air pollution and health. Retrieved from https://www.who.int/en/newsroom/factsheets/detail/ambient-(outdoor)-airquality-and-health.

Zakaria, N., & Azizah, R. (2013). Analysis of air pollution (SO_2), complaints of throat irritation and eye irritation health complaints on 64 food traders around Joyoboyo Terminal, Surabaya. *Jurnal K3, 2*(1).

Zhang, J. Y., Dai, H. X., Wu, Q. J., Li, J., Huang, Y. H., Chen, Z. J., Li, L. L., Chen, Y. L., Liu, S., & Jiang, C. Z. (2021). Maternal exposure to ambient levels of sulfur dioxide and risk of neural tube defects in 14 cities in Liaoning province, China: A population-based case-control study. *Journal of Exposure Science and Environmental Epidemiology, 31*(2), 266-275. https://doi.org/10.1038/s41370-020-00273-6.